DIRECTIONALLY SOLIDIFIED EUTECTICS AS HIGH TEMPERATURE FASTENERS

F. D. George
United Aircraft Research Laboratories
East Hartford, Connecticut

Abstract

In a number of laboratories, directionally solidified eutectics are being examined as candidate materials for vanes and blades in advanced gas turbines. Because of the superior high temperature properties displayed by two such alloys, a program was initiated to determine the suitability of these materials for high temperature fasteners.

Material properties pertinent to fastener applications were determined as a function of temperature. These properties included shear parallel and perpendicular to the growth direction and torsion parallel to the growth direction. Several techniques were investigated for fabricating typical fastener shapes. These fabrication methods included grinding, creep forming and direct casting. Finally, a brief evaluation of the performance of the best fabricated fastener design was made.

This study was funded by the National Aeronautics and Space Administration at Marshall Space Flight Center under contract No. NAS8-27358.

Introduction

In recognition of the current and anticipated requirements for superior high temperature materials, the Materials Laboratory of UARL has directed a substantial research effort in the establishment and evaluation of a technology for growing phase-reinforced eutectic alloys. The techniques used have demonstrated that materials with superior mechanical properties can be processed by the directional solidification of high temperature eutectic alloys. These investigations were prompted for the main purpose of developing an alloy for use in high temperature turbine applications. Several nickel and cobalt-based, phase-reinforced composite systems have been identified which display superior mechanical properties for temperatures to 2200°F. Certain of the characteristics, notably microstructural stability, tension, creep and fatigue, suggested that these type materials might qualify as high temperature fasteners for attaching thermal protection panels on space vehicles. For example, good microstructural stability would assure non-weakening of the fastener head area at the working temperatures and high creep resistance would prevent relaxation under load and help retain a "tight joint".

In comparison with other techniques for obtaining superior high temperature materials, the directionally solidified eutectic approach offers numerous advantages. One of the most important advantages is that a eutectic composite develops its reinforcing phase in situ by a one-step casting process. Since the composite structures are generated as a result of an equilibrium reaction, the phases produced are chemically stable with respect to one another. Furthermore, experience has shown that the low energy interfaces, established during the growth, result in a microstructure with exceptional stability which resists coarsening and spheroidization. Mechanically, as a first approximation, the behavior of these materials can be treated as normal composites. Recently it has been shown, however, that there is an important

effect of interphase spacing on strength. Reducing this spacing, which is accomplished by growing the material at a faster rate, has strengthened the material according to a Hall-Petch relationship. Thus, not only is processing benefited by rate increases but also properties.

Included in the disadvantages in the eutectic approach are anisotropic properties (as with other composites), a general inability to vary randomly the volume fraction of the phases, and some lack of freedom in selection of interesting systems. These last two disadvantages occur because we have selected to use a eutectic or eutectic-like composition where two or more phases crystallize simultaneously from a liquid. Even within these limitations, there are countless systems which can be anticipated if one considers ternary and higher order systems for study and development.

The prime material evaluated in this study was the directionally solidified Ni_3Al-Ni_3Cb eutectic alloy (1-5). After solidification the microstructure consists of a lamellar (sheet-like) dispersion of Ni_3Cb within a Ni_3Al matrix (Fig. 1). It contains approximately 44 volume percent of the Ni_3Cb reinforcing phase and the Ni_3Al matrix (a ductile intermetallic compound) is strengthened substantially by the 8 at. % columbium dissolved within it. The eutectic melting temperature is 2335°F and its density is 8.5 gm/cc. The alloy is a high modulus material whose tensile strength and creep-rupture strength are markedly superior to conventional superalloys. It is mildly notch sensitive at room temperature but is notch insensitive at elevated temperatures. Although it possesses low tensile ductility at room temperature, this does not mean the material is brittle. Its toughness is, in fact, comparable to superalloys at room temperature. The fatigue strength of the alloy is outstanding at room temperature, greatly surpassing that of nickel superalloys. This eutectic alloy exhibits such remarkable properties by virtue of the directional nature of its microstructure. The properties of the material are, as a consequence, directional. This material offers interesting possibilities for application as a high temperature fastener and if successfully developed, should satisfy performance requirements which cannot be met by conventional materials.

Since the Ni_3Al-Ni_3Cb alloy is representative of only one class of eutectic composites, i.e. the lamellar reinforced, a limited evaluation of the $(Co,Cr)-(Cr,Co)_7C_3$ eutectic (6-9) which is representative of the fibrous reinforced eutectic composite was also included in this program. This cobalt-based eutectic was modified by the addition of aluminum for the purpose of improving its oxidation resistance and to aid in stabilizing the cubic form of the cobalt in the alloy. The microstructure of this alloy is fibrous in nature (Fig. 1) and consists of approximately 26 volume percent of the carbide reinforcing phase with a cobalt, chromium, aluminum solid solution matrix. It has a density of 8.0 gm/cc and a melting temperature of 2370°F. Although not as strong as the Ni_3Al-Ni_3Cb eutectic alloy, the $(Co,Cr,Al)-(Cr,Co)_7C_3$ eutectic is more easily grown - rates of 50 cm/hr are typical - and is more oxidation resistant than the Ni_3Al-Ni_3Cb eutectic. This alloy is stronger than the conventional cast nickel-base superalloys in tension and creep and has comparable impact toughness. Because of the presence of the aligned fibrous carbide phase, it displays a high elastic modulus at room and elevated temperatures.

Other examples of "exotic" alloys which have been selected for study as candidate materials for potential use as high temperature structural fasteners include a dispersion strengthened metal TD NiCr (10) and these evaluations will be used for comparison purposes where possible.

Melting and Solidification Process

Master melts of eutectic composition were made in alumina crucibles and chill-cast in copper molds. The resulting bars were then placed in 1/2 inch diameter 99.7% recrystallized alumina cylindrical crucibles and unidirectionally solidified verti-cally within a resistively heated graphite tube furnace under a dynamic argon atmosphere (Fig. 2). These crucibles were held in a graphite sleeve which separated the crucible bottom from a water cooled brass pedestal by 1/4 inch of graphite. The crucibles were lowered from the furnace at rates corresponding to a nominal* solidi-fication velocity of 2 cm/hr for the Ni_3Al-Ni_3Cb eutectic and 10 cm/hr for the $(Co,Cr,Al)-(Cr,Co)_7C_3$ eutectic. Liquid superheats of approximately 500°F were employed and the thermal gradient in the liquid was estimated to have been 160°F/cm. Several 1/2 inch diameter ingots of both materials were formed as cast products by this vertical Bridgman-type directional solidification process. These ingots were then ground into test samples for the determination of the material properties pertinent to fastener application.

Material Property Evaluation Pertinent to Fastener Application

Transverse Shear

Bar samples rectangular in cross-section, 1/8 inch x 1/4 inch x 1 inch, were ground from the 1/2 inch diameter ingots with the direction of solidification parallel to the longest dimension so the strength in shear perpendicular (transverse) to the growth direction might be measured.

A double shear test fixture was used in this evaluation and initially the effect of span variations and the effect of the sample ends being clamped or free on the room temperature transverse shear strength were determined. High shear strength values were measured at short spans (0.010 inch) where the sample was supported in part by the anvil and lower apparent shear strengths were measured at longer spans (0.073 inch) where failure appeared to have occurred partly by bending. Samples tested at the intermediate span distances appeared to have failed in shear and the mean value was considered as the effective shear strength of the material at room temperature. There was little effect due to clamping the sample ends at the intermediate spans where shear failures were observed. Because of this all high temperature tests were run with free ends at a constant span (0.030 inch) within the intermediate range. The transverse shear tests were performed at a loading rate of 0.01 in./min.

In Fig. 3, a plot of effective shear stress vs. temperature indicates that the transverse shear strength of the Ni_3Al-Ni_3Cb eutectic is insensitive to temperature up to 1000°F. The transversely oriented Ni_3Al-Ni_3Cb displayed increasing ductility with temperature. The specimens pictured indicate the brittle failure at room tem-perature and the ductile behavior at 2200°F. The temperature dependence of transverse shear strength of the $(Co,Cr,Al)-(Cr,Co)_7C_3$ material is also shown in Fig. 3. This eutectic shows only a slight decrease in shear strength up to 1000°F and at that temperature exhibits a shear strength equivalent to that observed for the Ni_3Al-Ni_3Cb eutectic. Above this temperature, the shear strength drops off rather rapidly. The test specimens in Fig. 3 also show the increase in ductility with temperature. Finally,

---

*The failure to develop an exactly uniform rate of growth is primarily the result of the changing thermal gradient in the solid.

in Fig. 3, the shear strength values determined for 1/4 inch diameter specimens of TD NiCr (10) based on double shear testing are also shown. This dispersion strengthened metal which had been selected for study as a candidate material for potential use as a high temperature fastener yielded values that closely compare with those obtained for the fibrous $(Co,Cr,Al)-(Cr,Co)_7C_3$ eutectic.

Longitudinal Shear

Test specimens of both eutectic alloys for measuring longitudinal shear strength, shear parallel to the direction of solidification, were ground to shape and tested. These specimens consisted of a 1/4 inch diameter bolt shank with two 1/8 inch thick heads (one at each end of the shank) which were attached to a fixture composed of two high temperature slotted button-head adapters and split ring washers (to assure full bearing on the specimen heads). All longitudinal shear tests were run at a loading rate of 0.01 in./min and a shearing span distance of 0.010 inch.

The longitudinal shear strength values were determined using the diameter of the bolt shank in calculating the shear area. This approximation was used in the Ni_3Al-Ni_3Cb eutectic tests because the actual sheared area, as seen in Fig. 4, was not perfectly cylindrical which reflects the effect of the different orientations of the lamellae in the various grains sheared. A large amount of plasticity at the two higher temperatures is evident from the photographs in Fig. 4 of the specimens tested at these temperatures. The temperature dependence of longitudinal shear strength of the Ni_3Al-Ni_3Cb alloy is also shown in Fig. 4. An initial increase in longitudinal shear strength with an increase in temperature is evident. This increase is undoubtedly partly due to the increase in the flow stress of the Ni_3Al phase with temperature. This anomalous behavior has also been found in a $Ni_3(Al,Cb)$ single phase alloy, which is similar to the matrix phase of this eutectic, by Thornton, et al (11). The yield strength of this intermetallic compound increases with temperature up to approximately 1292°F.

The temperature dependence of longitudinal shear strength of the $(Co,Cr,Al)-(Cr,Co)_7C_3$ alloy is shown in Fig. 5. The photographs of fractured specimens at the various temperatures clearly indicate a transition from a tensile mode of failure to a shear mode of failure with increasing temperature. Although the failure mode of most of these specimens did not appear to be purely shear, the effective shear strength values were determined by using the bolt shank diameter in calculating the shear area.

Longitudinal Thread Shear

Longitudinal thread shear specimens 2 inches long with 1/4-20 threads at either end were ground from both eutectic ingots with the direction of solidification parallel to the long dimension. All longitudinal thread shear tests were run at a loading rate of 0.01 in./min. Because of the difficulty in determining the shear area in these test samples, several shadowgraphs were taken from different sides of the shear fracture surface and different areas were obtained. The shear strength values varied depending on the area used in the calculation and therefore an average value was used. In some more difficult cases, the values were calculated from shear areas determined from actual measurements (the width and length of thread sheared and the remaining sheared diameter).

The temperature dependence of longitudinal thread shear strength of the Ni_3Al-Ni_3Cb eutectic is shown in Fig. 6. Although the thread shear strength values obtained are higher than the values reported for the longitudinal shear strengths, the behavior

of both appears similar with respect to the materials response to temperature. The higher apparent thread shear strength values may be due to the difficulty in accurately determining the sheared area.

Although an increase in longitudinal shear strength with an increase in temperature was previously evident (Fig. 4), it is more dramatic in the longitudinal thread shear strength (Fig. 6). As previously mentioned, this is partly due to the increase in the flow stress of the Ni_3Al phase with temperature. This longitudinal shear strength increase in the thread tests may also be due in part to the increasing shear ductility which would allow more uniform engagement of the specimen threads and test adapter.

The temperature dependence of longitudinal thread shear strength of the (Co,Cr,Al)-$(Cr,Co)_7C_3$ eutectic is also shown in Fig. 6. The thread shear strength values obtained are higher than the values reported for the longitudinal shear strengths, but again the behavior of both appears similar with respect to the materials response to temperature. The higher apparent thread shear strength values may again be due to the difficulty in accurately determining the sheared area.

Torsion

Solid rods of the Ni_3Al-Ni_3Cb eutectic with gage sections of 0.125 inch diameter and either 2 inches or 1 inch long, with the long axis parallel to the growth direction, were fractured in torsion. These results are listed in Table 1.

Table 1

Torsional Strength of Ni_3Al-Ni_3Cb Eutectic Solidified at 2 cm/hr

Specimen Number	Temp. $^\circ$F	θ_{PL} deg.	τ_{PL} 10^3 psi	γ_{PL} %	G 10^6 psi	θ_f deg.	τ_f 10^3 psi	γ_f %
*A70-434-01	75	–	22	0.21	10.6	–	61	–
A71-749	75	6.9	42	0.76	–	113	72	12.3
*A70-434-02	400	–	27	0.29	9.2	~270	72	~15.2
A71-750	400	5.5	39	0.61	–	159	74	17.4
A71-751	1000	6.9	47	0.76	–	299	84	32.7
A72-339	1600	5.9	25	0.64	–	529	48	57.8
A72-338	2200	1.7	4	0.19	–	889	16	97.0

strain measured by a time scale which was converted to an angle of twist measurement
gage length = 1 inch
rate of applied torque = .67 RPM

G = shear modulus
τ_{PL}, τ_f = shear stresses at proportional limit and at failure
γ_{PL}, γ_f = shear strains at proportional limit and at failure
θ_{PL}, θ_f = angle of twist at proportional limit and at failure
* = strain measured by bonded strain gages oriented in the direction of the principal stress (gage length = 2 inches)

The following equations were used in determining the values shown in Table 1 for the two strain gaged specimens.

Shear stress at proportional limit* $\tau_{PL} = Tr/J$ (1)

Shear strain at proportional limit* $\gamma_{PL} = 2\epsilon\,(2/G.F.)$ (2)

Shear modulus** $G = Tr/J\gamma$ (3)

Shear stress at failure $\tau_f = 3\,M_f/2\pi\,r^3$ (4)

where $T \equiv$ torque
$r \equiv$ radius of gage section
$J \equiv$ polar moment of inertia $(\pi D^4/32)$, $D \equiv$ diameter of gage section
$\epsilon \equiv$ strain output measurement
$G.F. \equiv$ strain gage factor
$M_f \equiv$ torsional moment or torque at failure

Shear stress values given for specimens where strain was measured by a time scale which was then converted to an angle of twist measurement (θ) were determined using Eqs. (1) and (4) for the shear stress at the proportional limit and at failure respectively. The shear strain values for these specimens at the proportional limit and at failure were calculated using the following equation:

$$\gamma = r\theta/L \qquad (5)$$

where $r \equiv$ radius of gage section
$\theta \equiv$ angle of twist
$L \equiv$ length of gage section

There is an appreciable difference in both the shear stress and shear strain values at the proportional limit for specimens tested under the same conditions depending on the method used for measuring strain. This difference, however, is substantially reduced when these values are compared at the point of failure. The approximate shear strain value given in Table 1 for specimen number A70-434-02 was determined using Eq. (5) and a visual measurement of the angle of twist after failure.

The torque vs angle of twist curves for the Ni_3Al-Ni_3Cb alloy are shown in Fig. 7. The three curves, room temperature, 400°F and 1000°F, essentially vary only in the degree of twist at failure which increases with increasing temperature. For these temperatures, characteristic of cold working, the torque increased continuously with angle of twist up to a maximum where the specimen separated. Also, the specimen tested at 1000°F experienced cracking, as noted in Fig. 7, well before final failure occurred. The initial cracking was recorded at an angle of twist of 67.1 degrees. Using Eqs. (4) and (5), the shear stress and shear strain at crack initiation were calculated to be 56 x 10^3 psi and 7.3% respectively. For temperatures characteristic

---

*Proportional limit is defined as the point where the shear-stress and shear-strain curve first deviates from linearity.
**Shear modulus is determined from the slope of the linear portion of the shear-stress, shear-strain curve.

of hot working, (e.g. 1600 and 2200°F) the torque reached a peak and then gradually fell until the specimen fractured. For the 1600°F test, this peak occurred at an angle of twist of 467 degrees, a maximum shear stress of 51×10^3 psi and a shear strain of 51%. The peak for the 2200°F test occurred at an angle of twist of 559 degrees and a shear stress and shear strain of 18×10^3 psi and 61% respectively. The corresponding fractured specimens at room temperature (brittle fracture) and 2200°F (ductile failure) are also shown in Fig. 7.

Solid rods of the $(Co,Cr,Al)-(Cr,Co)_7C_3$ eutectic with a gage section of 0.125 inch diameter and 1 inch long, with the long axis parallel to the growth direction, were fractured in torsion. These results are given in Table 2.

Table 2

Torsional Strength of $(Co,Cr,Al)-(Cr,Co)_7C_3$ Eutectic Solidified at 10 cm/hr

Specimen Number	Temp. °F	θ_{PL} deg.	τ_{PL} 10^3 psi	γ_{PL} %	G 10^6 psi	θ_f deg.	τ_f 10^3 psi	γ_f %
*A71-771D	75	–	33	0.27	12.0	–	–	–
A71-771D	75	6.9	56	0.76	–	126	89	13.8
*A71-771E	400	–	25	0.20	12.2	–	–	–
A71-771E	400	6.9	50	0.76	–	88	77	9.6
A72-012A	1000	7.6	56	0.83	–	268	89	29.3
A72-004E	1650	2.1	9	0.23	–	349	10	38.1

Refer to Table 1 for footnotes

The same equations described previously were used to determine the values listed in Table 2 for this fibrous eutectic. The appreciable difference in shear stress and strain at the proportional limit for specimens tested under the same conditions but with different strain measuring methods is also present in these results.

The torque vs angle of twist curves for the $(Co,Cr,Al)-(Cr,Co)_7C_3$ alloy are shown in Fig. 8. Again, as in the previous eutectic alloy study, the torque at temperatures up to and including 1000°F increased with increasing angle of twist until it reached a maximum where the specimen failed. Only during the 1650°F test did the torque increase to a peak and then decrease before the specimen fractured. This peak occurred at an angle of twist of 320 degrees, a maximum shear stress of 15×10^3 psi and a shear strain of 35%. Why the angle of twist at failure was less at 400°F than at room temperature is not presently understood. Also, the specimen tested at 1000°F experienced cracking, as noted in Fig. 8, well before final failure. The initial cracking was recorded at an angle of twist of 72.7 degrees. Using Eqs. (4) and (5), the shear stress and shear strain at crack initiation were calculated to be 70×10^3 psi and 7.9% respectively. The corresponding fractured specimens at room temperature (brittle fracture) and 1650°F (ductile failure) are also shown in Fig. 8.

Fabricating Techniques

Grinding

All the test specimens for determining the material properties pertinent to fastener application of both eutectic alloys were successfully fabricated by grinding.

A typical flush head fastener shape of the Ni_3Al-Ni_3Cb eutectic that was fabricated by grinding is shown in Fig. 9. The direction of solidification is parallel to the long axis of the fastener. Various lamellar orientations, all parallel to the growth direction, are evident from the two microstructural views in Fig. 9. Several double flush headed specimens were ground to shape from Ni_3Al-Ni_3Cb ingots directionally solidified at 2 cm/hr for use in evaluating this process as a method for fabricating fasteners.

Casting

Two mold designs were used for the purpose of determining the feasibility of directly casting the Ni_3Al-Ni_3Cb eutectic into a typical flush head fastener shape. One design allowed directional solidification to proceed from the fastener shank to the flush head and the other allowed directional solidification from the flush head shape into the shank. Figure 10 shows two eutectic ingots that were successfully solidified at 2 cm/hr using both of these designs. The center photographs in Fig. 10 show the ingots after removal from the high purity alumina mold in which they were directionally cast. There appears to be no indication of a metal-mold reaction. The outermost photographs show the cast fastener shapes after macro-etching their surfaces. It is evident from the grain alignment seen in these photographs that the solidification was directional.

A double flush headed specimen of the Ni_3Al-Ni_3Cb eutectic that was cast into shape at 2 cm/hr is shown in Fig. 11. The top photograph shows the ingot after removal from the high purity alumina mold in which it was directionally cast. Again, there appears to be no indication of a metal-mold reaction. Microstructural examination of the views shown in Fig. 11 indicates a relatively gradual transition of the eutectic grain alignment through the two flush headed shapes of the cast ingot.

A few single and double 100° flush headed specimens of the Ni_3Al-Ni_3Cb eutectic were directionally cast in order to evaluate this process as a method of fabricating fasteners.

Creep Forming

Bar samples 0.250 inch diameter by approximately 2 inches long, of both the Ni_3Al-Ni_3Cb and the $(Co,Cr,Al)-(Cr,Co)_7C_3$ eutectics were ground with the direction of solidification parallel to the long dimension. Several attempts were made to hot forge the ends of these samples with a 100° flush head die. The two major problems encountered were the lack of temperature control and the high strain rate which in some cases caused the material to shatter. A hot forging temperature of approximately 2200°F was selected but often the sample temperature fell well below this level and in other instances some melting of the sample was evident.

These initial experiments led to the belief that a creep forming process where temperature and strain rate can be better controlled, may prove worthwhile in producing a satisfactory flush head fastener shape. Bar samples, 0.250 inch diameter by approximately 1.7 inches long, of both eutectics were ground with the direction of solidification parallel to the long dimension. Both alloys were successfully creep formed into a flush head fastener shape (Figs. 12, 13 and 14) using a molybdenum die. The forming was accomplished in vacuum at 2200°F at a rate of approximately 0.015 inch per minute and a pressure of approximately 25×10^3 psi. The 100° flush head formed was 0.40 inch in diameter and 0.06 inch high. No distortion occurred, the materials completely filled the die, and there was no problem with die release as the difference in thermal expansion between the die material and the alloys being formed automatically provides adequate clearance on cooling. Metallographic examination indicated favorable phase distribution and flow in the flush head area of both alloys (Figs. 13 and 14).

Several specimens were fabricated to determine the shear strength of these eutectic materials when made into a typical fastener shape using the creep forming process.

Evaluation of Fabricated Fasteners

The material properties pertinent to fastener applications which have been determined for both the lamellar Ni_3Al-Ni_3Cb and the fibrous $(Co,Cr,Al)-(Cr,Co)_7C_3$ directionally solidified eutectic alloys are encouraging and indicate that these alloys show promise as candidate materials for high temperature fastener applications.

A $100°$ countersunk flush head design was chosen as a typical fastener shape for the evaluation of fabricated fasteners because this configuration is common in the assembly of skin panels to substructures where a flush surface is required.

Room Temperature Shear Strength

The longitudinal thread shear results for both eutectics indicated that shearing of threads was not a major problem. This study revealed that with adequate thread engagement (more than two threads) failure would occur either by shear or tension at the fastener head or by tension through the root of the thread. With this knowledge and because of the directional nature of these eutectic microstructures which are affected by the processing method, the shear strength evaluation of fabricated fasteners was centered around the determination of the effective shear strength of the fastener heads only.

The results of the room temperature shear strength evaluation of $100°$ flush head fastener shapes of the Ni_3Al-Ni_3Cb eutectic for the three fabrication techniques are listed in Table 3. The double headed specimen configurations were tested in the same manner as described in the longitudinal shear strength determinations. The single headed fastener configurations were tested using a V-type wedge grip with serrated faces which clamped around the shank of the fastener.

Table 3

Room Temperature Shear Strength Evaluation of $100°$ Flush Head Fastener
Shape of Ni_3Al-Ni_3Cb Eutectic Solidified at 2 cm/hr

Specimen Number	Fabrication Technique	Specimen Configuration	Effective Shear Stress psi	Failure Mode
A71-735A	ground	double headed	37,200	Shear & Tensile
A71-735B	ground	double headed	26,400	Shear & Tensile
A72-217	cast	double headed	24,000	Tensile
A72-237	cast	double headed	23,400	Shear & Tensile
A72-217a	cast	single headed	20,000	Shear & Tensile
A71-692	cast	single headed	31,200	Shear & Tensile
A71-694	cast	single headed	26,300	Shear & Tensile
A71-461-02	creep formed	single headed	14,900	Tensile (cellular microstructure)
A71-493-1	creep formed	single headed	31,600	Tensile (lamellar microstructure)

Most of the effective shear stress values listed in Table 3 compare favorably with those plotted in Fig. 4 with the following exceptions, the higher value of 37,200 psi for the double headed ground specimen and the lower value of 14,900 psi for the creep formed specimen. This low value can be explained by the fact that microstructural examination after testing revealed that the specimen contained a cellular microstructure near the fastener head. This local breakdown in the lamellar microstructure could cause a weakening of the material in that area when exposed to 2200°F during the forming process.

A limited evaluation of the $(Co,Cr,Al)-(Cr,Co)_7C_3$ eutectic is given in Table 4. These specimens were all creep formed and the first two tested yielded values that compare closely to the values plotted in Fig. 5 which were determined using ground specimens. The third test of a creep formed specimen resulted in a much higher effective shear stress than the previous two. These results are quite encouraging and indicate that a more concentrated study into the feasibility of a thermal mechanical working process as a fabricating technique for eutectic materials should be continued.

Table 4

Room Temperature Shear Strength Evaluation of 100° Flush Head Fastener
Shape of $(Co,Cr,Al)-(Cr,Co)_7C_3$ Eutectic Solidified at 10 cm/hr

Specimen Number	Fabrication Technique	Specimen Configuration	Effective Shear Stress psi	Failure Mode
#1	creep formed	single headed	42,600	Tensile
#2	creep formed	single headed	45,700	Tensile
#3	creep formed	single headed	68,800	Tensile

Effect of Flush Head Angle on Room Temperature Shear Strength

Double flush headed specimens of the Ni_3Al-Ni_3Cb eutectic which were ground to shape, were tested to determine the effective longitudinal shear strength (shear parallel to the direction of solidification) at room temperature of this material as a function of flush head angle. The effect of flush head angle on the room temperature longitudinal shear strength of this alloy is shown in Fig. 15. The influence of higher compressive forces perpendicular to the tapered surface are evident by the increase in the effective shear strength with a decrease in flush head angle.

All room temperature shear strength evaluation tests were performed at a loading rate of 0.01 in./min and the fastener shank diameter (0.250 inch) and height of fractured head were used in calculating the shear area.

Effect on Room Temperature Torsional Strength after Exposure at 2200°F

Directionally solidified ingots of both the Ni_3Al-Ni_3Cb and $(Co,Cr,Al)-(Cr,Co)_7C_3$ eutectics were prepared and ground into torsion specimens for room temperature torsional tests after exposure at 2200°F for 30, 60, and 120 minutes. These results are shown in Tables 5 and 6. Little or no effect can be seen on the room temperature torsional strength after exposure at 2200°F in the Ni_3Al-Ni_3Cb eutectic whereas a slight effect is evident in the $(Co,Cr,Al)-(Cr,Co)_7C_3$ alloy.

Table 5

Effect on the Room Temperature Torsional Strength of Ni_3Al-Ni_3Cb Eutectic
Solidified at 2 cm/hr after Exposure at 2200°F

Specimen Number	Exposure Time min	θ_{PL} deg.	τ_{PL} 10^3 psi	γ_{PL} %	θ_f deg.	τ_f 10^3 psi	γ_f %
A71-749	0	6.9	42	0.76	113	72	12.3
A72-180	30	6.6	44	0.72	121	70	13.2
A72-336	60	6.6	39	0.72	131	78	14.3
A72-196	120	6.9	47	0.76	120	72	13.1

strain measured by a time scale which was converted to an angle of twist measurement
gage length = 1 inch
rate of applied torque = .67 RPM

τ_{PL}, τ_f ≡ shear stresses at proportional limit and at failure
γ_{PL}, γ_f ≡ shear strains at proportional limit and at failure
θ_{PL}, θ_f ≡ angle of twist at proportional limit and at failure

Table 6

Effect on the Room Temperature Torsional Strength of $(Co,Cr,Al)-(Cr,Co)_7C_3$
Eutectic Solidified at 10 cm/hr after Exposure at 2200°F

Specimen Number	Exposure Time min	θ_{PL} deg.	τ_{PL} 10^3 psi	γ_{PL} %	θ_f deg.	τ_f 10^3 psi	γ_f %
A71-771B	0	6.9	56	0.76	126	89	13.8
A72-009D	30	5.2	39	0.57	166	92	18.1
A72-009E	60	5.9	36	0.64	175	84	19.1
A72-004F	120	6.8	45	0.74	225	96	24.6

Refer to Table 5 for footnotes

Shear-Rupture

    Directionally solidified ingots of the Ni_3Al-Ni_3Cb eutectic alloy were prepared
and ground into double headed longitudinal shear specimens for short-term stress-
rupture testing. The specimen design used was the same as described in the
longitudinal shear strength determinations. The resulting data are plotted in Fig. 16
and are compared with longitudinal-rupture data obtained for this eutectic from a
previous study (1) and with thread-rupture data for TD NiCr (10).

Conclusions

    The present program has revealed that both the lamellar Ni_3Al-Ni_3Cb and the
fibrous $(Co,Cr,Al)-(Cr,Co)_7C_3$ directionally solidified eutectic alloys show promise
as candidate materials for high temperature fastener applications. Although no tor-
sion data were available for comparison, the transverse shear values obtained for
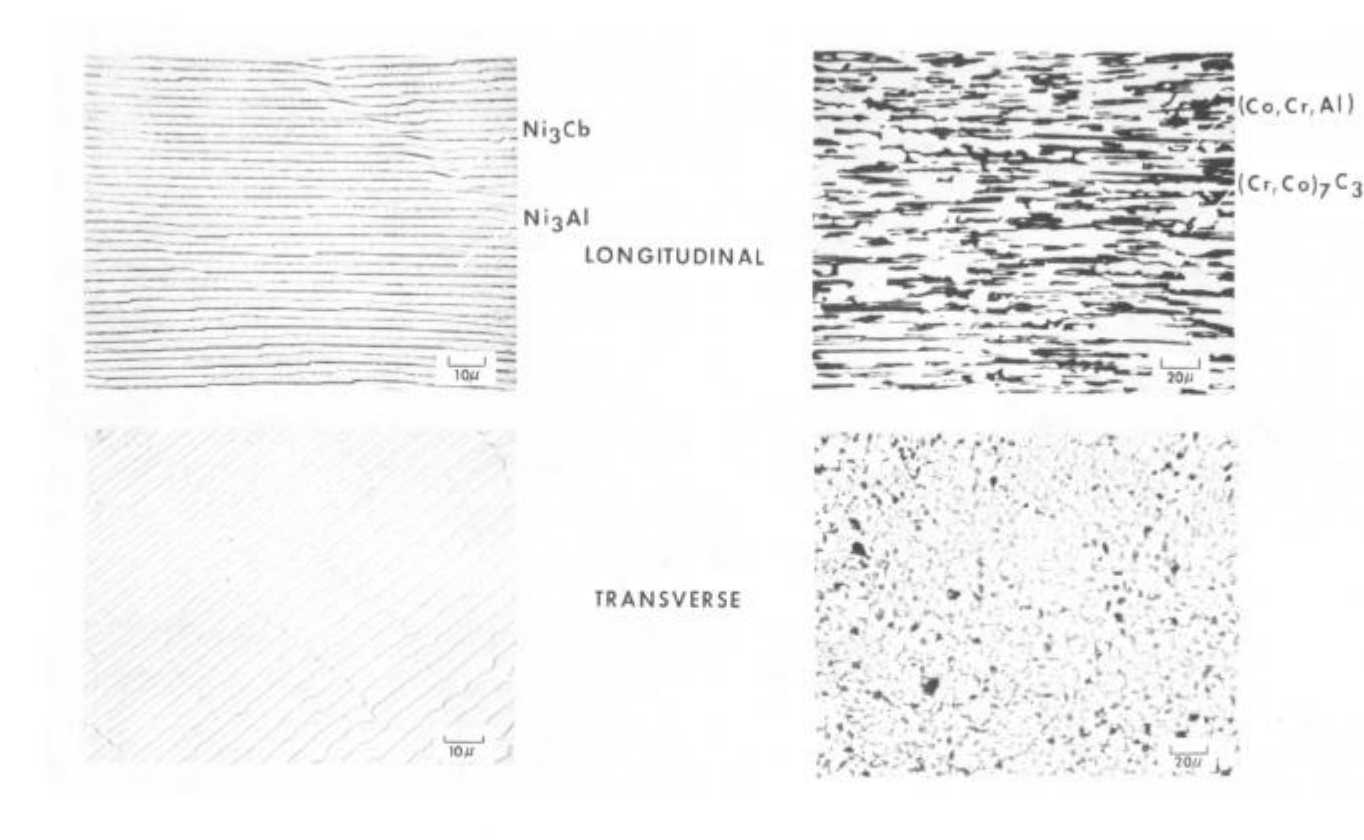both eutectic alloys (based on double shear testing) indicated equal or higher

strengths than that reported for dispersion strengthened metals (e.g. TD NiCr) which were selected in a previous study for potential use as structural fasteners. The stress-rupture characteristics of the Ni_3Al-Ni_3Cb eutectic compare favorably with that of TD NiCr considering the difference in the testing mode used in obtaining the data. Finally, this study has indicated that a eutectic material can be successfully formed to shape by grinding, casting, and thermal-mechanical working (creep forming).

Acknowledgements

References

1.   Thompson, E. R. and F. D. George: Investigation of the Structure and Properties of the Ni_3Al-Ni_3Cb Eutectic Alloy. Final Report, Contract N00019-69-C-0162 (July 31, 1969).

2.   Thompson, E. R. and F. D. Lemkey: Structure and Properties of $Ni_3Al(\gamma')$-Based Eutectic Alloys. ASM Trans. Quarterly, Vol. 62, pp 140-154 (1969).

3.   Thompson, E. R. and F. D. George: Eutectic Superalloys. 1969 SAE Transactions, Vol. 78, p 2283 (Dec. 1970).

4.   Thompson, E. R., F. D. George, and E. H. Kraft: Investigation to Develop a High Strength Eutectic Alloy with Controlled Microstructure. Final Report, Contract N00019-70C-0052 (July 31, 1970).

5.   Thompson, E. R., E. H. Kraft, and F. D. George: Investigation to Develop a High Strength Eutectic for Aircraft Engine Use. Final Report, Contract N00019-71-C-0096 (July 31, 1971).

6.   Thompson, E. R. and F. D. Lemkey: Unidirectional Solidification of Cobalt-Chromium-Carbon Monovariant Eutectic Alloys. Met. Trans. Vol. 1, p 2799 (1970).

7.   Thompson, E. R., D. A. Koss, and J. C. Chesnutt: Mechanical Behavior of a Carbide Reinforced Cobalt-Chromium Eutectic Alloy. Met. Trans., Vol. 1, p 2807 (1970).

8.   Lemkey, F. D. and E. R. Thompson: Nickel and Cobalt Eutectic Alloys Reinforced by Refractory Metal Carbides. Met. Trans., Vol. 2, p 1537 (1971).

9.   Thompson, E. R.: Anisotropic Toughness of a Carbide Reinforced Cobalt, Chromium Eutectic. J. Composite Mat., Vol. 5, p 235 (1971).

10.   Roach, T. A.: Dispersion Strengthened Metals Structural Mechanical Fastener Evaluation. Tech. Report AFFDL-TR-68-89 (June 1968).

11.   Thornton, P. H., R. G. Davies, and T. L. Johnston: The Temperature Dependence of the Flow Stress of the γ' Phase Based Upon Ni_3Al. Met. Trans., Vol. 1, p 207 (1970).

Figure 1. Microstructure of Unidirectionally Solidified Ni_3Al-Ni_3Cb and (Co,Cr,Al)-$(Cr,Co)_7C_3$ Eutectics
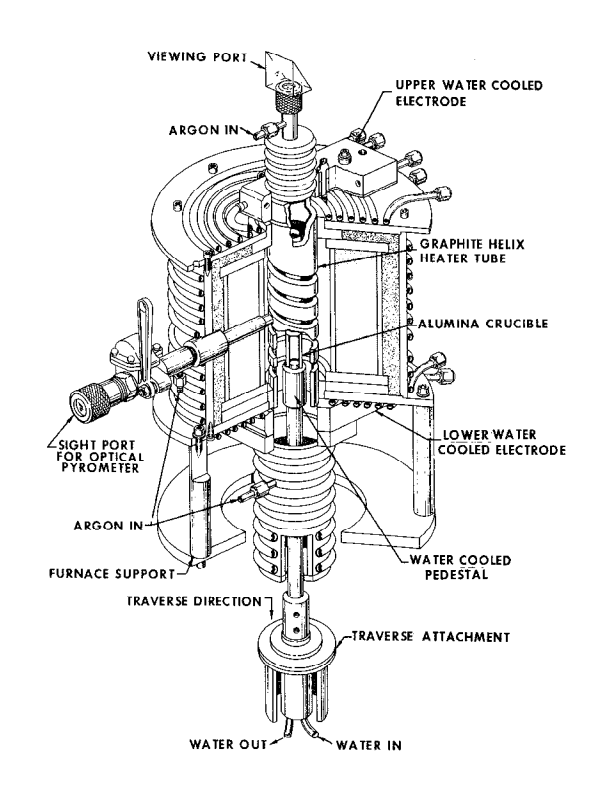
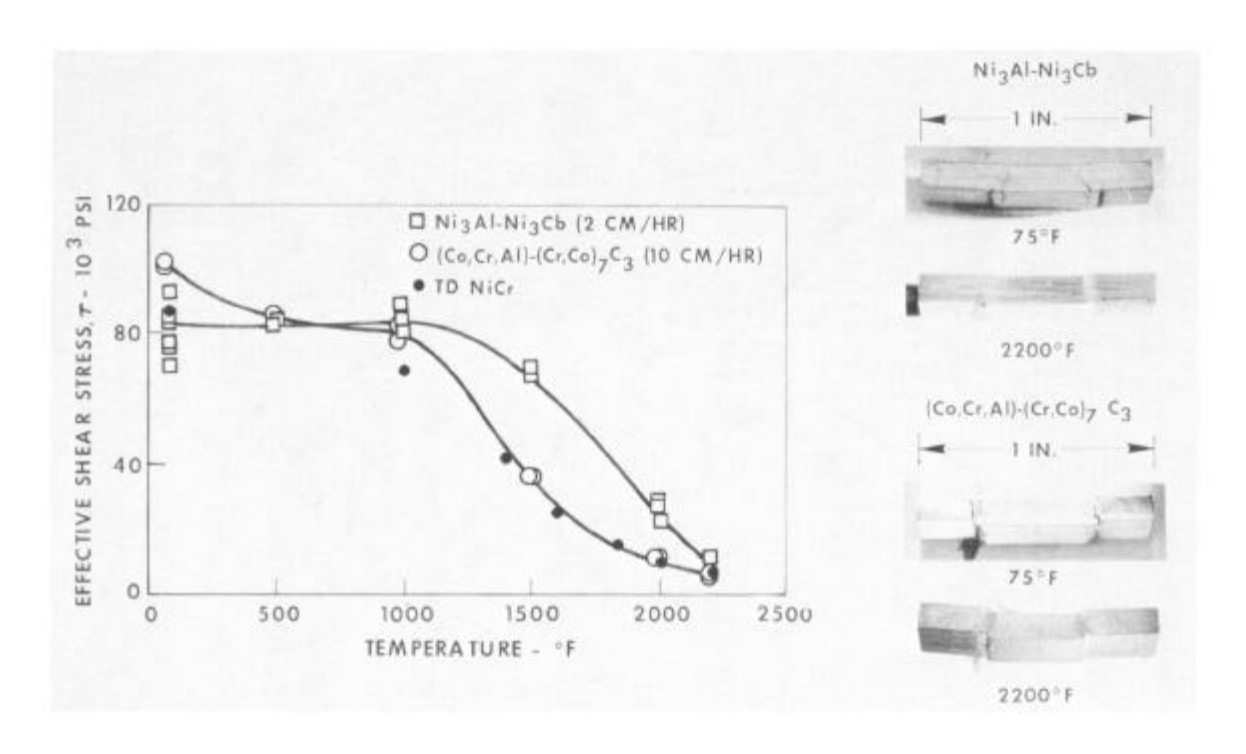Figure 2. Graphite Directional Solidification Furnace

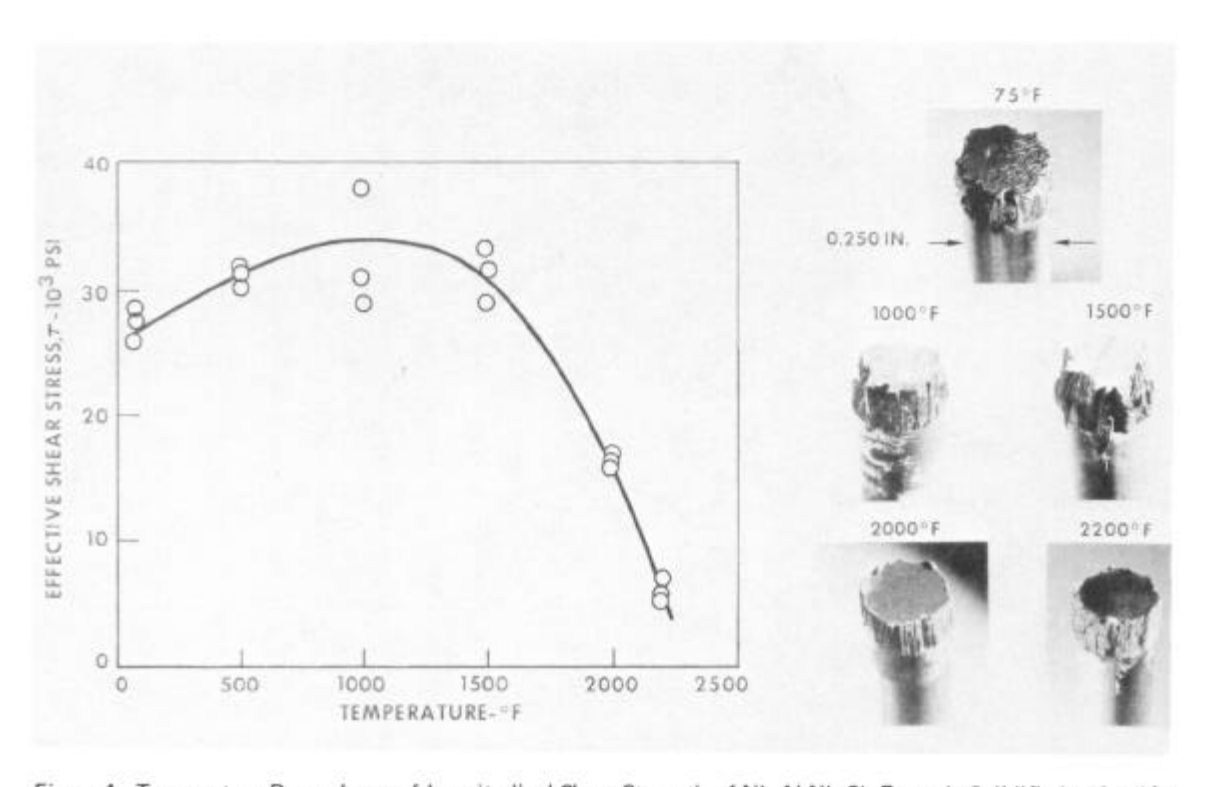Figure 3. Temperature Dependence of Transverse Shear Strength

Figure 4. Temperature Dependence of Longitudinal Shear Strength of Ni_3Al-Ni_3Cb Eutectic Solidified at 2 cm/hr
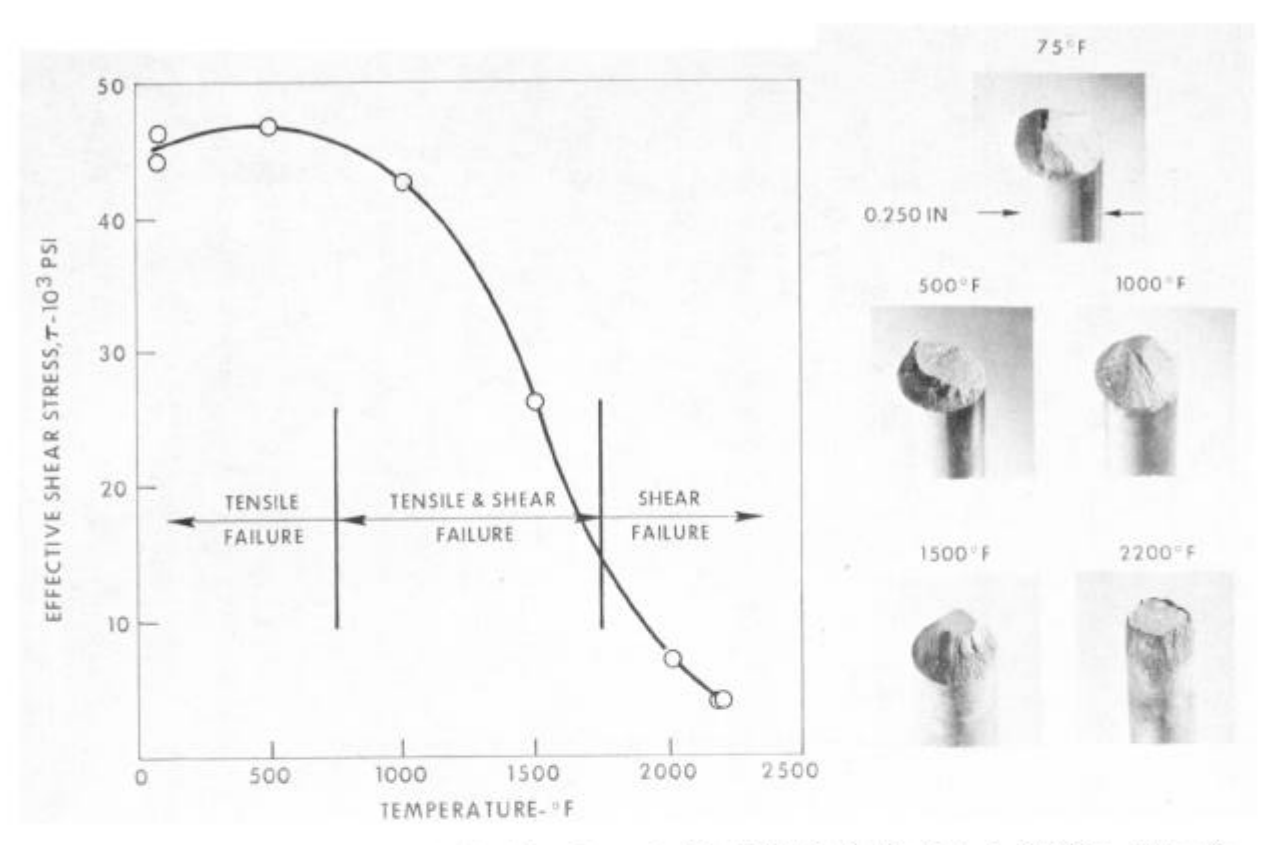
Figure 5. Temperature Dependence of Longitudinal Shear Strength of $(Co,Cr,Al)-(Cr,Co)_7C_3$ Eutectic Solidified at 10 cm/hr
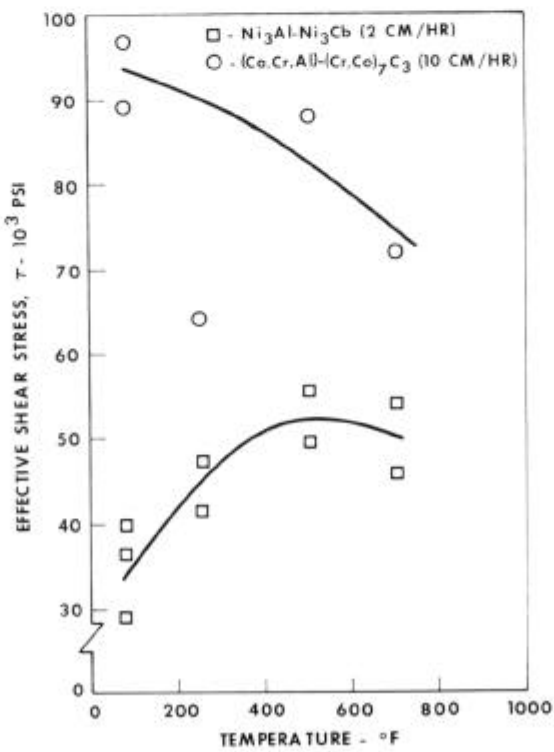

Figure 6. Temperature Dependence of Longitudinal Thread Shear Strength
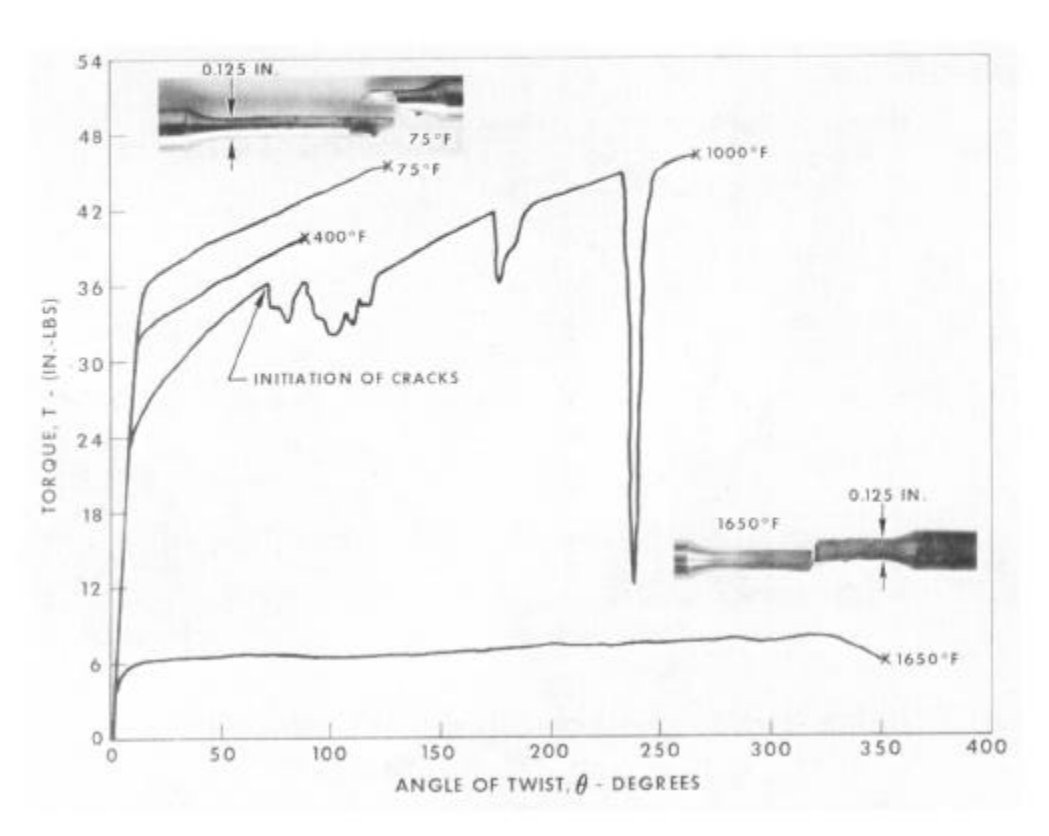
Figure 7. Torque vs Angle of Twist for Ni$_3$Al-Ni$_3$Cb Eutectic Solidified at 2 cm/hr
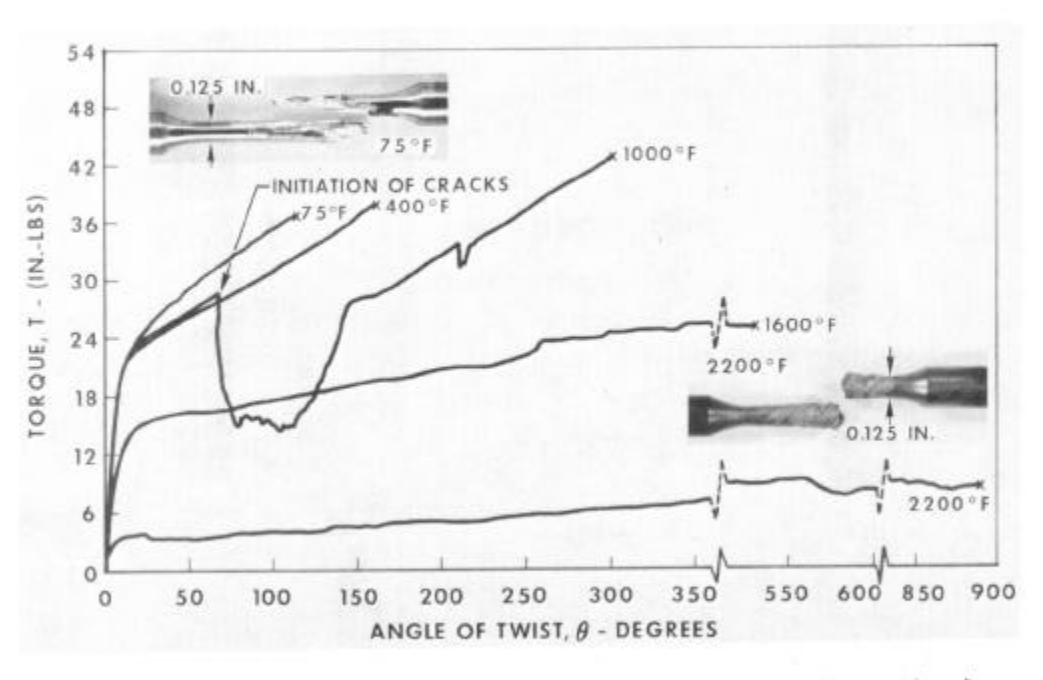
Figure 8. Torque vs Angle of Twist for (Co,Cr,Al)—(Cr,Co)$_7$C$_3$ Eutectic Solidified at 10 cm/hr
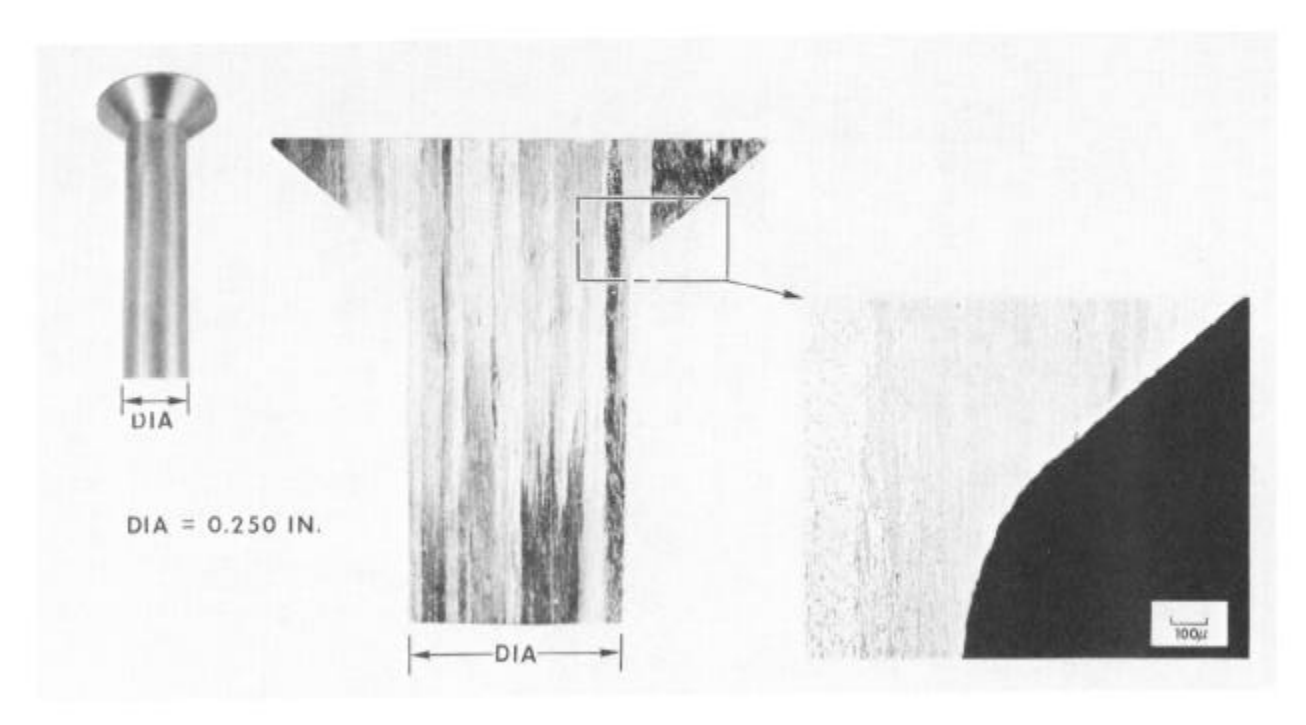
Figure 9. Ground Flush Head Fastener Shape of the Ni_3Al-Ni_3Cb Eutectic
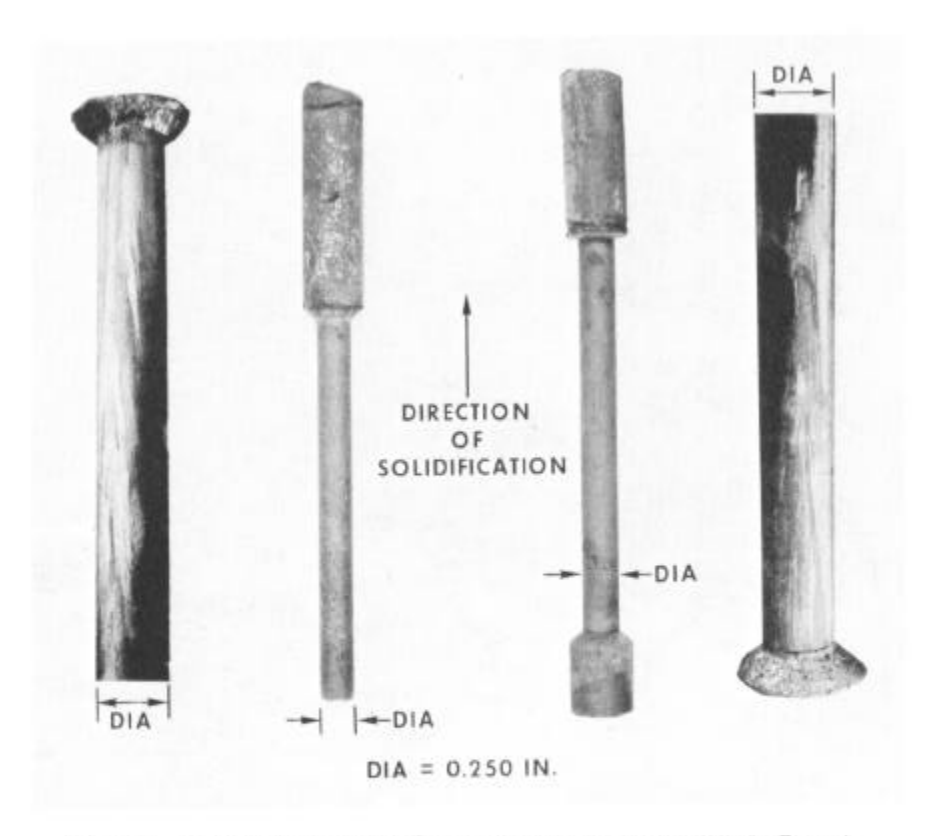
Figure 10. Cast Single Flush Head Fastener Shapes of the Ni_3Al-Ni_3Cb Eutectic
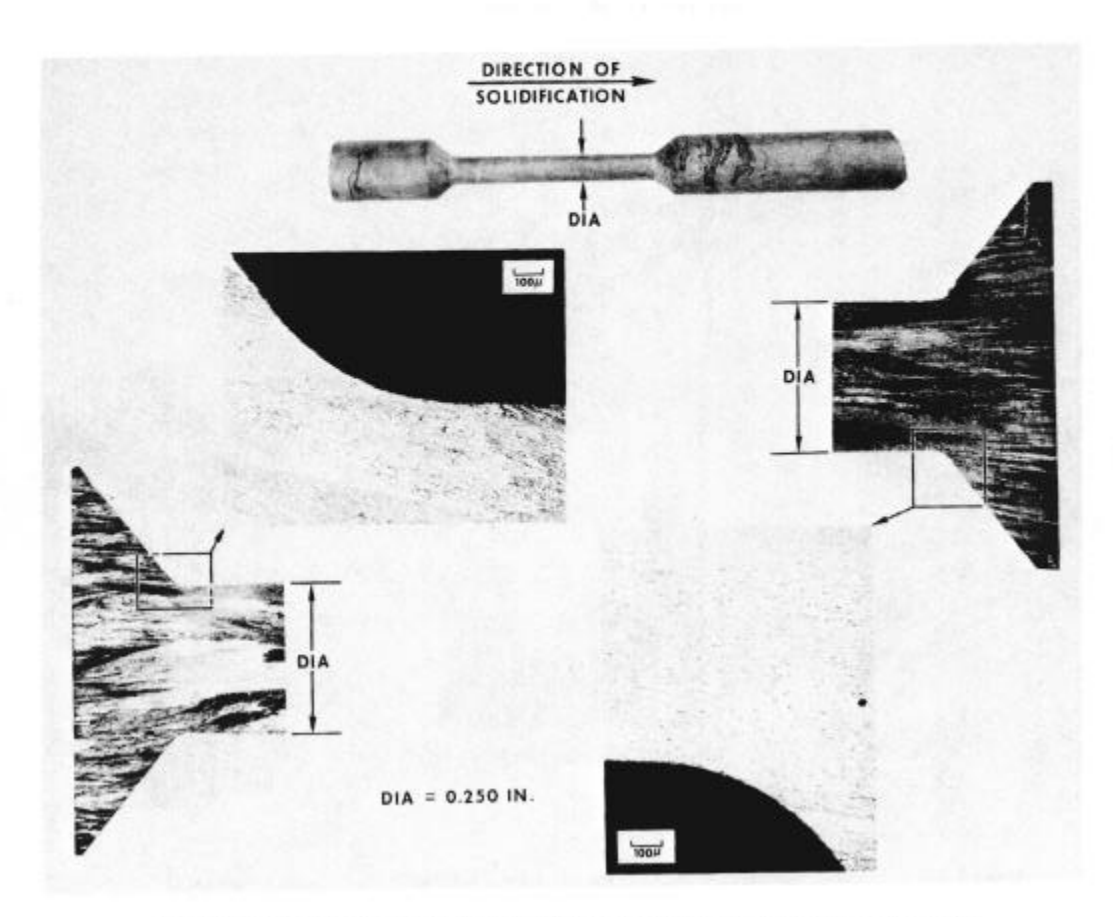
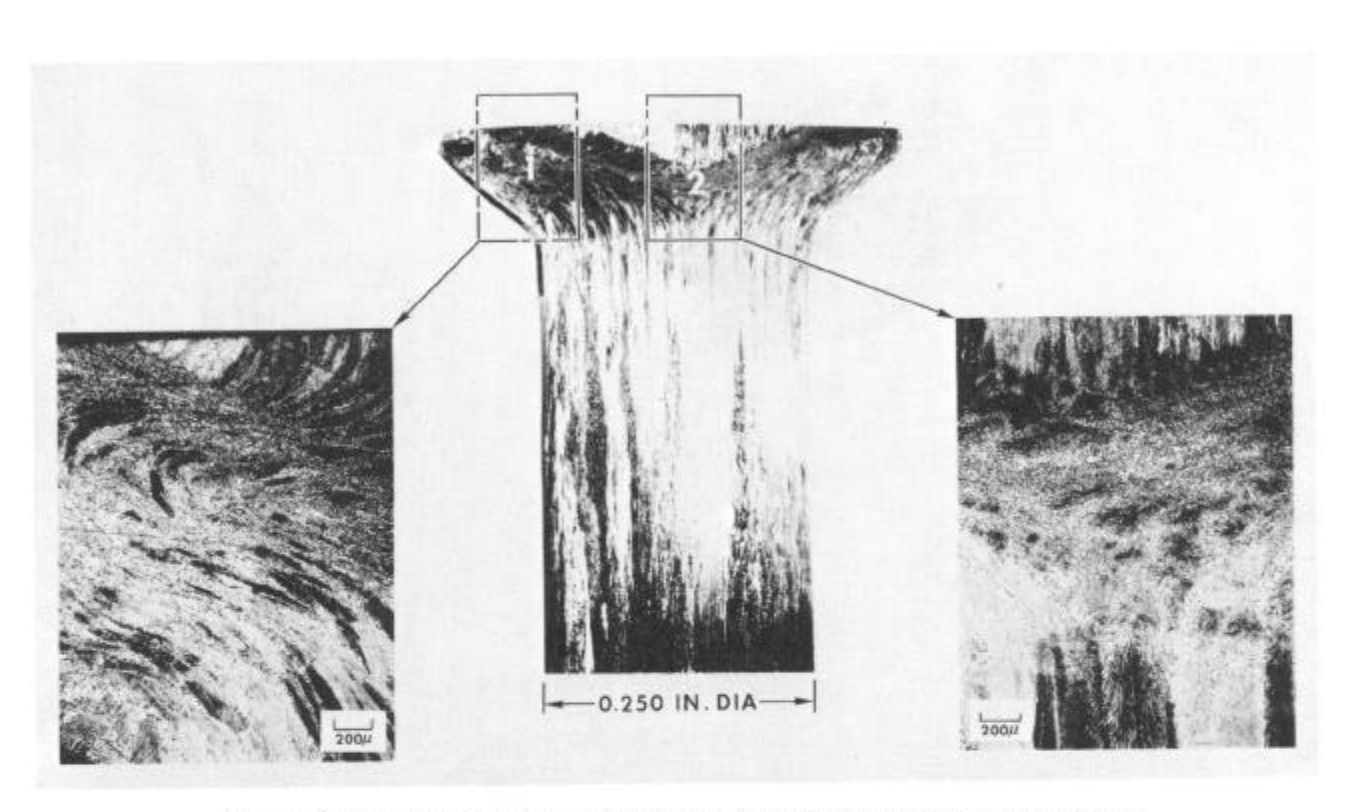Figure 11. Cast Double Flush Head Fastener Shape of the Ni_3Al-Ni_3Cb Eutectic
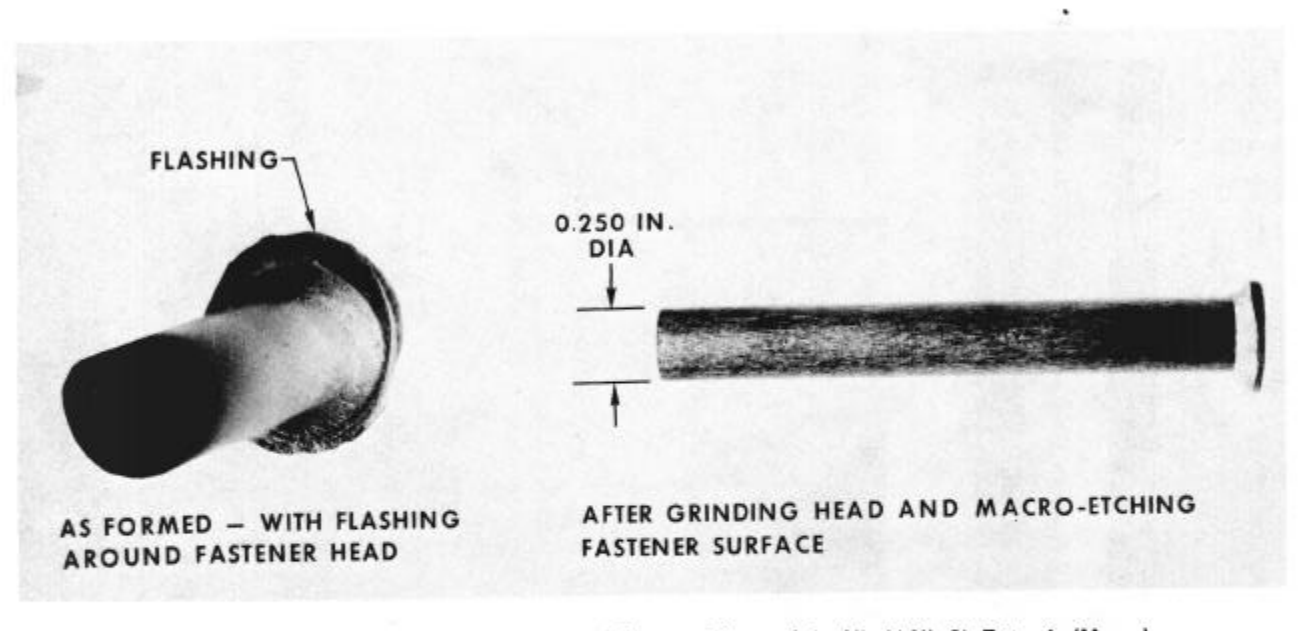
Figure 12. Creep Formed Flush Head Fastener Shape of the Ni_3Al-Ni_3Cb Eutectic (Macro)

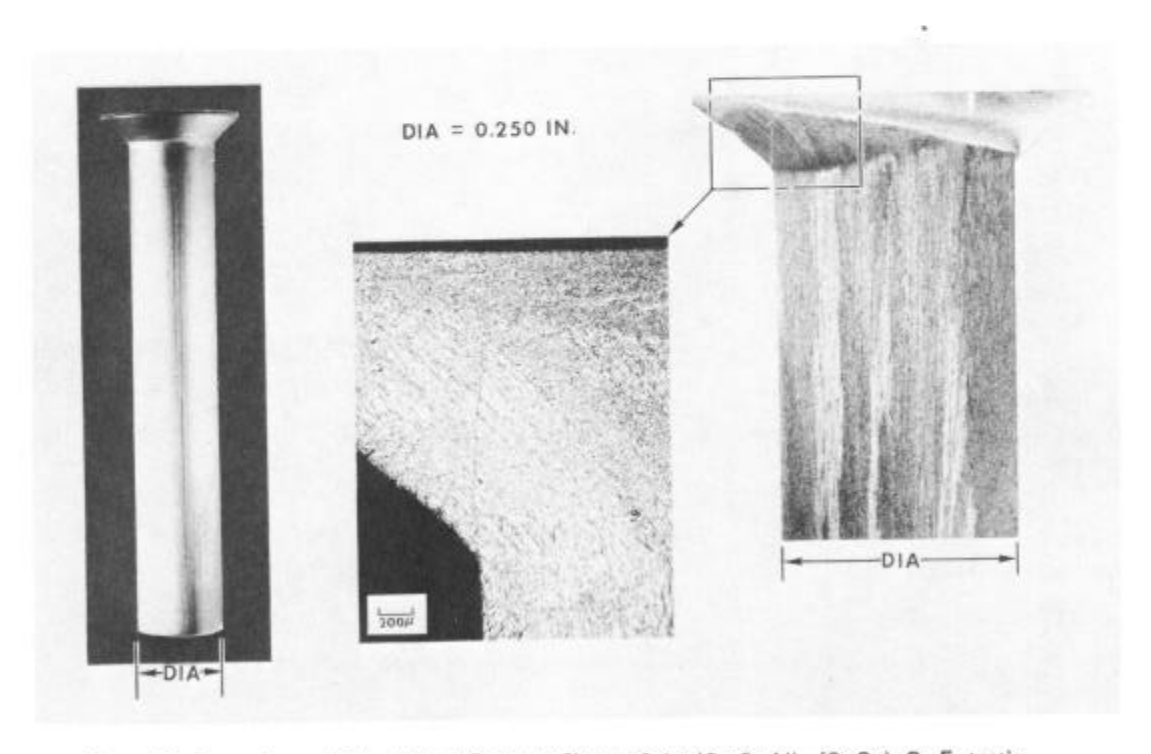Figure 13. Creep Formed Flush Head Fastener Shape of the Ni_3Al-Ni_3Cb Eutectic (Micro)

Figure 14. Creep Formed Flush Head Fastener Shape of the $(Co,Cr,Al)-(Cr,Co)_7C_3$ Eutectic
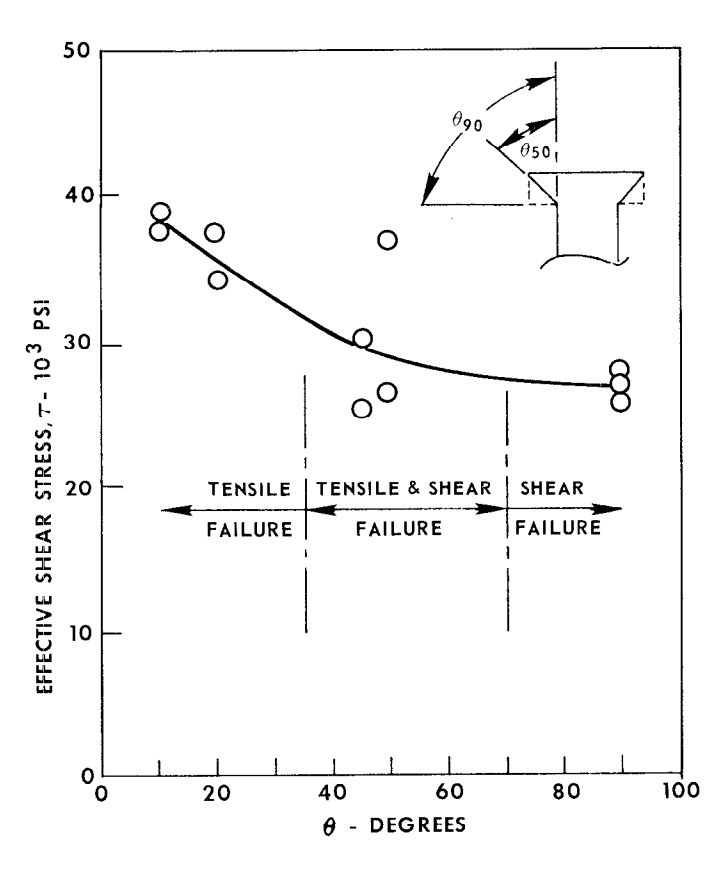
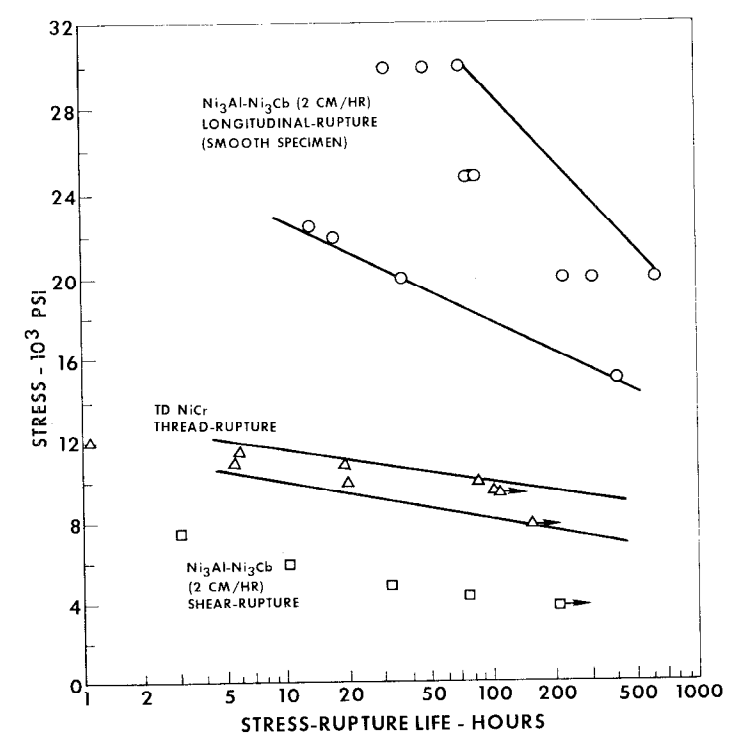Figure 15. Room Temperature Shear Strength Evaluation of Ground Fastener Shapes of Ni_3Al-Ni_3Cb Eutectic Solidified at 2 cm/hr

Figure 16. Stress-Rupture Life vs Stress at 2000 F